Acta Geod Geophys (2015) 50:391–402
DOI 10.1007/s40328-015-0099-3

Coherence spectra of rotational and translational components of mining induced seismic events

Alexey A. Lyubushin · Zdeněk Kaláb · Markéta Lednická · Jaromír Knejzlík

Received: 17 September 2014 / Accepted: 15 January 2015 / Published online: 28 January 2015

Abstract Classical Russian S-5-S pendulum seismometer was modified for recording of the rotational components of ground motion. This seismometer was used for monitoring of mining induced seismic events in the Karviná region (Czech Republic). Together, three translational components of ground vibration velocity and one rotational component of ground vibration velocity around the vertical axis were recorded. Elaborated mining induced seismic events with epicentral distances up to 9 km were recorded in Doubrava locality, where the exploitation of black coal is still active. Numerical study of measured component attributes of mining induced seismic events is presented in this paper, namely squared Morlet wavelet coefficients and squared coherence spectrum between rotational and translational components. Squared Morlet wavelet coefficients enable to analyse time-and-frequency structure of elaborated signal, e.g. dynamics of the onset, evolution and disappearance of typical periods of the harmonic peaks, etc. Spectral measure of coherence was applied here for investigation of synchronization effects in 2-dimensional time series of translational and rotational components.

Keywords Rotational component · Squared Morlet wavelet coefficient · Coherence spectrum · S-5-SR seismometer · Mining induced seismicity

1 Introduction

It is necessary for full description of the ground vibration, in addition to three translational components and strain, to consider also three rotational components (e.g., Båth 1979; Teisseyre et al. 2006). Traditionally, only the translational components of the earthquake ground vibration and structural response have been recorded. Classical Russian pendulum S-5-S seis-

A. A. Lyubushin
Institute of the Physics of the Earth, RAS, Moscow, Russia

Z. Kaláb (✉) · M. Lednická · J. Knejzlík
Institute of Geonics ASCR, Ostrava, Czech Republic
e-mail: kalab@ugn.cas.cz

mometer was modified for recording of the rotational components of ground motion (Knejzlík et al. 2012). This S-5-SR seismometer was used for mining induced seismic events monitoring in the Karviná region that is located in northern part of Moravia, the Czech Republic (e.g., Martinec et al. 2006). Used data were recorded in Doubrava locality, where the exploitation of black coal and mining induced seismicity is still active. Analysis of measured translational components of mining induced seismic events in time and frequency domain was published in e.g. Častová and Kaláb (1997), Lyubushin et al. (2004a), Kaláb et al. (2011), Kaláb and Knejzlík (2011). Results of performed analyses are important especially for vibration effect evaluation on the surface in inhabited areas (Kaláb and Lednická 2012; Lednická 2006; Hradil et al. 2009).

First records of rotational component of ground vibration velocity in the Karviná region were obtained during the experimental seismic monitoring in 2010 and 2011 that confirmed rotational component existence also for the mining induced seismic events (Kaláb et al. 2013). The maximum measured value of rotational velocity exceeded value of 1 mrad s^{-1} at Doubrava locality (mining induced seismic event with epicentral distance 1 km and energy 5.3 E^5 J).

In this paper, records of mining induced seismic events originated in the Ostrava–Karviná Coalfield are used to present analysis of selected attributes of translational and rotational components, namely squared Morlet wavelet coefficients and squared coherence spectrum between rotational and translational components. Three more intensive events (seismic energy range $2.5E^5$–$2.8E^6$ J) were selected to present result of performed numerical study. Epicentral distances of elaborated events range from 3 to 9 km (Fig. 1). Evaluation of more distant events with epicentral distances longer than 10 km is not representative for the coherence spectra analysis due to quickly attenuated value of rotational velocity (Kaláb et al. 2013).

Three translational components of ground vibration velocity (Z, N, E) and one rotational component of ground vibration velocity around the vertical axis (Rot) were recorded on surface solitaire seismic station in Doubrava locality performed by Institute of Geonics, ASCR Ostrava. Digital instrument PCM3-EPC was used for measurement of rotational component of ground vibration velocity (Knejzlík and Kaláb 2002). The data have been recorded in a trigger mode using 100 Hz sampling frequency, which is sufficient in relation to the frequency range of used S-5-SR seismometer. The measurement of translational components of ground vibration velocity was performed by the digital mobile seismic station GAIA in continual recording mode with sampling frequency of 100 Hz. The frequency range of used three-component seismometer ViGeo2 was 2–200 Hz, which is sufficient compared to prevailing frequency range of evaluated mining induced seismic events with epicentral distance up to 10 km.

2 S-5-SR seismometer

The S-5-SR seismometers recording rotational components of ground vibrations around the vertical axis (Fig. 2) and around the horizontal axis were developed at the Institute of Geonics ASCR (Knejzlík et al. 2012). Laboratory tests of the S-5-SR seismometer were carried out to obtain information about the new seismometer behaviour and to calibrate its basic parameters. A test vibration table, that is located at the Geophysical Institute of the ASCR, Prague, was used. Both translational and rotational movements of the table is possible to set up. Natural period of pendulum was set-up to 5 s and system was optimally damped.

To obtain maximum accuracy of measurement, an output signal from the seismometer was analysed using Brüel & Kjær Spectral Analyzer Type 2031. Output signal levels

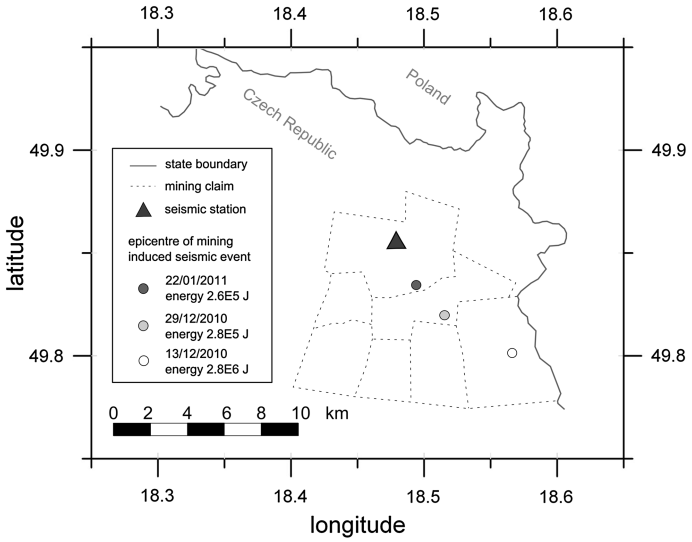

Fig. 1 Localization of seismic station and localization of epicentres of analysed mining induced seismic events

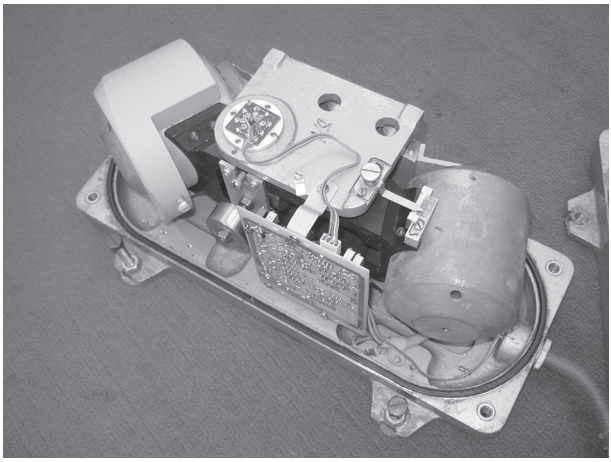

Fig. 2 The S-5-SR seismometer recording rotational components of ground vibrations around the vertical axis (photo: Lednická)

for rotational and translational excitations of S-5-SR seismometer are presented on Fig. 3. Sensitivity constant for angular velocity $k(d\varphi/dt) = 52.6$ V s rad^{-1} was obtained and sensitivity constant $k(\varphi) = 1393$ V rad^{-1} was set for an angular displacement channel. Sensitivity $kp = 1.1$ mV Hz^{-1} was taken for a parasitic sensitivity on a translational oscillation perpendicular to the pendulum and its rotational axis on stationary amplitude 50μm (peak-peak). As a result, $k(d\varphi/dt)$ to kp ratio is better than 40 dB within frequency range 0.2–25 Hz. Due to non-linearity of sensing electrodynamic transducer and limited amplitude of damping feedback signal, the range of measured amplitudes is limited to 10 mrads^{-1}. Sensitivity is limited by noise level 1.1 μrads^{-1} below 0.5 Hz (Kaláb and Knejzlík 2012).

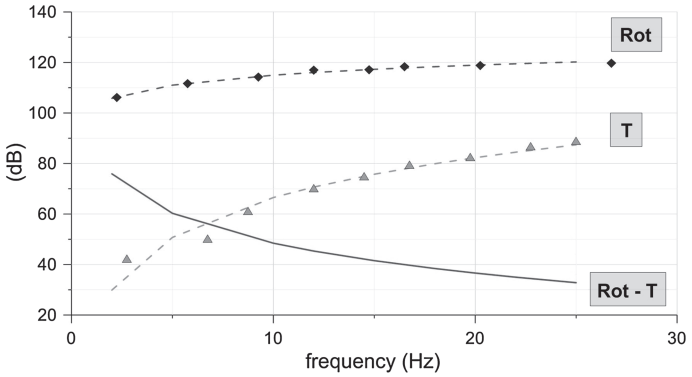

Fig. 3 Output signal levels for rotational (R) and translational (T) excitations of S-5-SR seismometer. In both cases double amplitude of vibrations was 50 μm. R–T curve represents attenuation of translational component

3 Continuous Morlet wavelet transform diagrams

Let $x(t)$ is the times series being analysed. We are interested in its time-and-frequency structure. A continuous wavelet analysis is the most sensitive tool for the purpose (Chui 1992; Daubechies 1992; Mallat 1998). Let $\psi(t)$ is a certain function satisfying the admissibility condition: $\int_{-\infty}^{+\infty} \psi(t)dt = 0$ and the normality condition: $\int_{-\infty}^{+\infty} |\psi(t)|^2 dt = 1$. A value which depends on two parameters $((t, a),\ a > 0)$ is called a continuous wavelet transform:

$$Wx(t,a) = \frac{1}{\sqrt{a}} \int_{-\infty}^{+\infty} x(s) \cdot \psi\left(\frac{s-t}{a}\right) ds = \sqrt{a} \int_{-\infty}^{+\infty} x(t+av) \cdot \psi(v)\, dv \qquad (1)$$

Here t—is the time point, $a > 0$—is the scale parameter, which we will further give a more usual term as "period". The value (1) reflects behaviour of the signal under study about a point $\boldsymbol{t}$ with a typical period of variations a. It is reasonable that the value (1) depends greatly on the choice of the function $\psi(t)$. Further we will use the so-called Morlet wavelet or a complex-valued modulated Gaussian:

$$\psi(t) = \frac{1}{\pi^{1/4}} \exp(-t^2/2 - i\pi t) \qquad (2)$$

This wavelet is adapted best of all for distinguishing short-lived harmonic peaks (trains) and has certain optimality properties in the search of a compromise between the frequency and time resolution (yielding the so-called Heisenberg limit). Our aim is to construct a two-dimensional map of the squared module of value (1) $\log_{10}(|Wx(t,a)|^2)$, which gives a pictorial presentation of the dynamics of the onset, evolution and disappearance of typical periods of the harmonic peaks of the signal under study.

4 Spectral measure of coherence

Here we apply spectral measure of coherence $\lambda(\tau, \omega)$ which was suggested in (Lyubushin 1998) for multidimensional time series processing in the problems of geophysical monitoring. This spectral measure was applied for investigating synchronization effects in multidi-

mensional time series in hydrology (Lyubushin et al. 2004b, c), seismology (Lyubushin and Sobolev 2006; Lyubushin 2008, 2009, 2010, 2014) and climate researches (Lyubushin and Klyashtorin 2012). Here we use it in the particular case of 2-dimesional time series. In general case $\lambda(\tau, \omega)$ is constructed as the module of the product of component-by-component canonical coherences

$$\lambda(\tau, \omega) = \prod_{j=1}^{m} |\nu_j(\tau, \omega)| \tag{3}$$

Here, $m \geq 2$ is the total number of jointly analysed time series; ω is frequency; τ is the time coordinate of the right-hand end of the moving time window consisting of a definite number of adjacent samples; and $\nu_j(\tau, \omega)$ is the canonical coherence of the j-th scalar time series, which describes the strength of coupling of this series with all other series. The quantity $|\nu_j(\tau, \omega)|^2$ is the generalization of the ordinary squared spectrum of coherence between two signals for the case, when the second signal is not scalar but vector. The inequality $0 \leq |\nu_j(\tau, \omega)| \leq 1$ is fulfilled, and the closer the value of $|\nu_j(\tau, \omega)|$ to unity, the stronger the linear relation of variations at the frequency ω in the time window with the coordinate τ of the j-th series to analogous variations in all other series.

For calculating the measure (3) it is necessary to estimate spectral matrix $S(\tau, \omega)$ of the size $m \times m$ within each time window with time coordinate τ. For this purpose we use vector autoregression model (Marple 1987):

$$Z(t|\tau) + \sum_{k=1}^{p} A_k(\tau) \cdot Z(t-k|\tau) = e(t|\tau) \tag{4}$$

where t is time index within current time window with time coordinate τ, $Z(t|\tau)$ is the piece of m-dimensional time series corresponding to the current time window, p is an autroregression order, $A_k(\tau)$ are matrices of autoregression coefficients of the size $m \times m$, $e(t|\tau)$ is m-dimensional residual signal with zero mean and covariance matrix $\Phi(\tau) = M\{e(t|\tau)e^T(t|\tau)\}$. Matrices $A_k(\tau)$ and $\Phi(\tau)$ are defined in each time window using Durbin-Levinson procedure and the spectral matrix is calculated using formula:

$$S(\tau, \omega) = F^{-1}(\tau, \omega) \cdot \Phi(\tau) \cdot F^{-H}(\tau, \omega), \qquad F(\tau, \omega) = E + \sum_{k=1}^{p} A_k(\tau) \cdot \exp(-i\omega k) \tag{5}$$

where E is a unit matrix of the size $m \times m$, "H" is the sign of Hermitian conjunctions.

We applied the measure (3) for the case when $m = 2$ within time window of the length 200 samples with mutual shift 10 samples after coming to increments of waveforms. We used autoregression order $p = 5$ in the formula (4).

In general case when $m > 2$ the value (3) is calculated using canonical coherences of the m-dimensional time series $Z(t)$ (Lyubushin 1998), but for our particular case when $m = 2$ the value (3) equals to $|S_{12}(\tau, \omega)|^2 / (S_{11}(\tau, \omega) \cdot S_{22}(\tau, \omega))$, where $S_{11}(\tau, \omega)$ and $S_{22}(\tau, \omega)$ are diagonal elements of the matrix (5), i.e. parametric estimates of the power spectra of two signals within time window with time coordinate τ, and $S_{12}(\tau, \omega)$ is their mutual cross-spectrum.

5 Results and discussion

Analysis of squared Morlet wavelet coefficients and squared coherence spectrum between rotational and translational components is presented using three mining induced seismic

events with epicentral distances about 3 km (22/01/2011), 5 km (29/12/2010) and 9 km (13/12/2010). Epicentres of all three mining induced seismic events were located in south-east direction of Doubrava seismic station. Calculated attributes are evaluated in the frequency range from 2 to 25 Hz, which results from the frequency range of used sensors ViGeo2 and S-5-SR. This frequency range is sufficient for analysis of mining induced seismic events with epicentral distance up to 10 km, because prevailing frequency range of elaborated mining induced seismic events lies within this range.

According the wave patterns on Figs. 4, 5 and 6, it is possible to see that rotational components for all three elaborated events are clear defined; so it is possible to elaborate its time-frequency diagrams and perform coherence spectra analysis between rotational and translational components. Duration of main phase of rotational motion is similar as for translational component. Maximum values of rotational components are not at the same time as for the translational components.

For all translational and rotational components, squared Morlet wavelet coefficients were calculated to analyse time-and-frequency structure of elaborated signal, e.g. dynamics of the onset, evolution and disappearance of typical periods of the harmonic peaks, etc. In diagrams of squared Morlet wavelet coefficients, red–yellow colours emphasize main frequency range of elaborated mining induced seismic event. For example, undistinguished onset of P-wave on "29/12" event is more clearly depicted in figure of wavelet coefficients than in the wave pattern (Fig. 5). According the results, prevailing frequency range of all components of all three events is from 3 to 10 Hz. The higher range reaches only vertical component of the nearest "22/01"event, namely 4.5–16 Hz for P-wave. The lower range reaches horizontal components in north-south direction (N component), namely 2–5.5 Hz for "22/01" event and 1.6–5.5 Hz for "29/12" event.

For investigation of synchronization effects in 2-dimensional time series of translational and rotational components, time-frequency diagrams of evolution of the squared coherence spectrum for 3 pairs of components "Rot, Z", "Rot, N" and "Rot, E" were elaborated. The estimates were performed within moving time window of the length 2 s, therefore first point of time axis is 2 s and it represents attribute of whole elaborated time of moving time window (below signed as rh-time).

The nearest "22/01" event (Fig. 4) shows high coherences in short interval with frequency range 10–20 Hz on the rh-time 2.5–3 s, which corresponds to P-wave phase. For the S-wave phase, there is practically no synchronization effects between rotational and translational components. It is possible to see some coherence only for "Rot, E" components with range of frequencies 7–17 Hz, especially in rh-time 3.5–6 s. During whole elaborated time starting from rh-time 6 s it is possible to document slight coherence with frequency value about 4.5–6 Hz for all components.

Second "29/12" event (Fig. 5) can be characterized by high coherences in the rh-time 3–5 s in frequency range 5–10 Hz, which correspond to S-wave phase of the event. During whole elaborated time starting from rh-time 8 s it is possible to document slight coherence with frequency value about 4–5 Hz. Higher coherences in the rh-time 13–15 s with frequency about 30–35 Hz are not sufficiently explained and are out of the elaborated frequency range 2–25 Hz.

The most distant "13/12" event (Fig. 6) can be characterized by significant coherences in the rh-time 3–10 s with frequency range 5–10 Hz. The most significant coherence is documented for "Rot, E" components in the rh-time 4.5–6 s, which corresponds to S-wave phase of the event. Higher coherences in the rh-time about 8 s with frequency range 20–45 Hz were also detected, but these frequencies are out of evaluated range 2–25 Hz. Also for this event, it is possible to document slight coherence with frequency value about 4.5–5.5 Hz

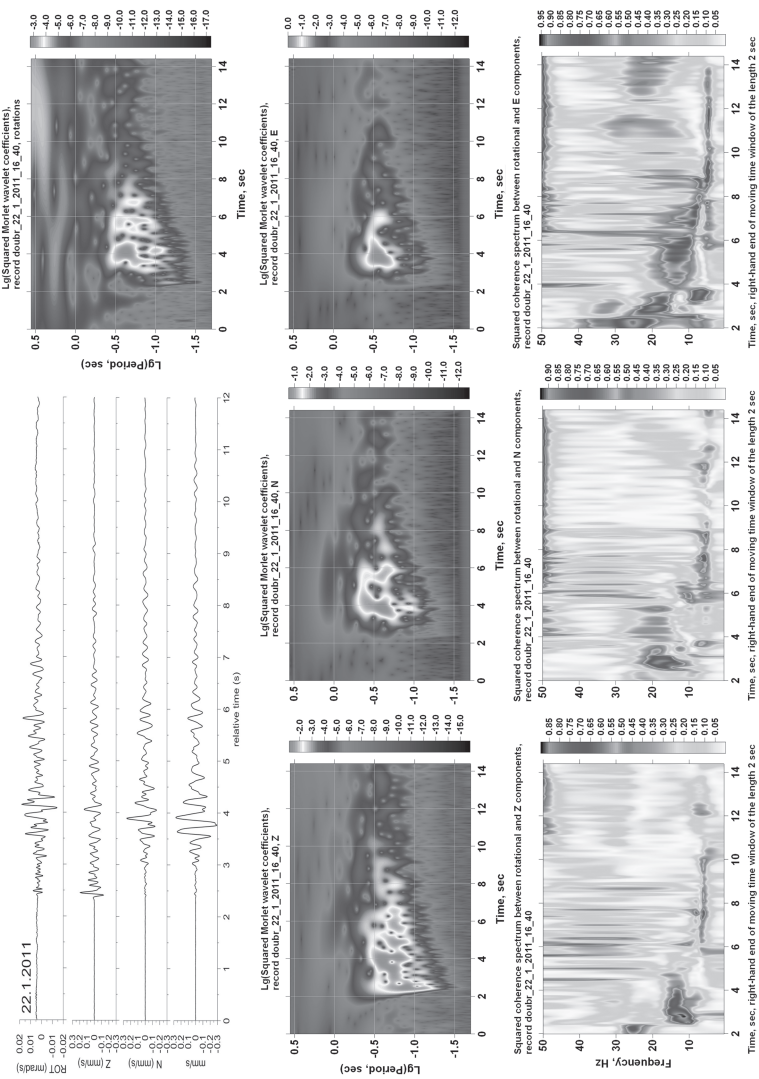

Fig. 4 Example of elaboration of "22/01" seismic event from Karviná region (for details see text). Left-above Rotational component of ground vibration velocity around the vertical axis and translational components of ground vibration velocity (down from top vertical, horizontal N-S, horizontal E-W components); Right-above and second row Squared Morlet wavelet coefficients of individual components; down row Time-frequency diagrams of evolution of the squared coherence spectrum (moving time window of the length 2 s)

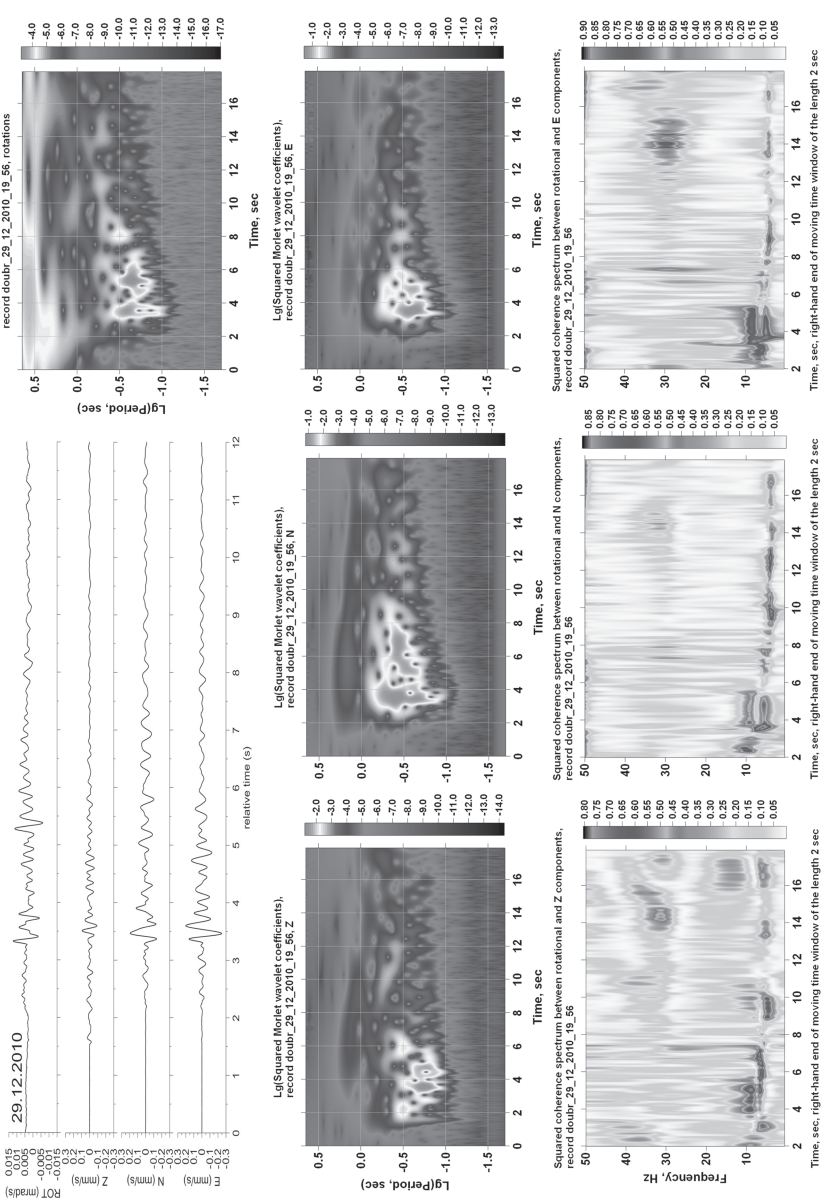

Fig. 5 Example of elaboration of "29/12" seismic event from Karviná region (for details see text and comment to Fig. 4)

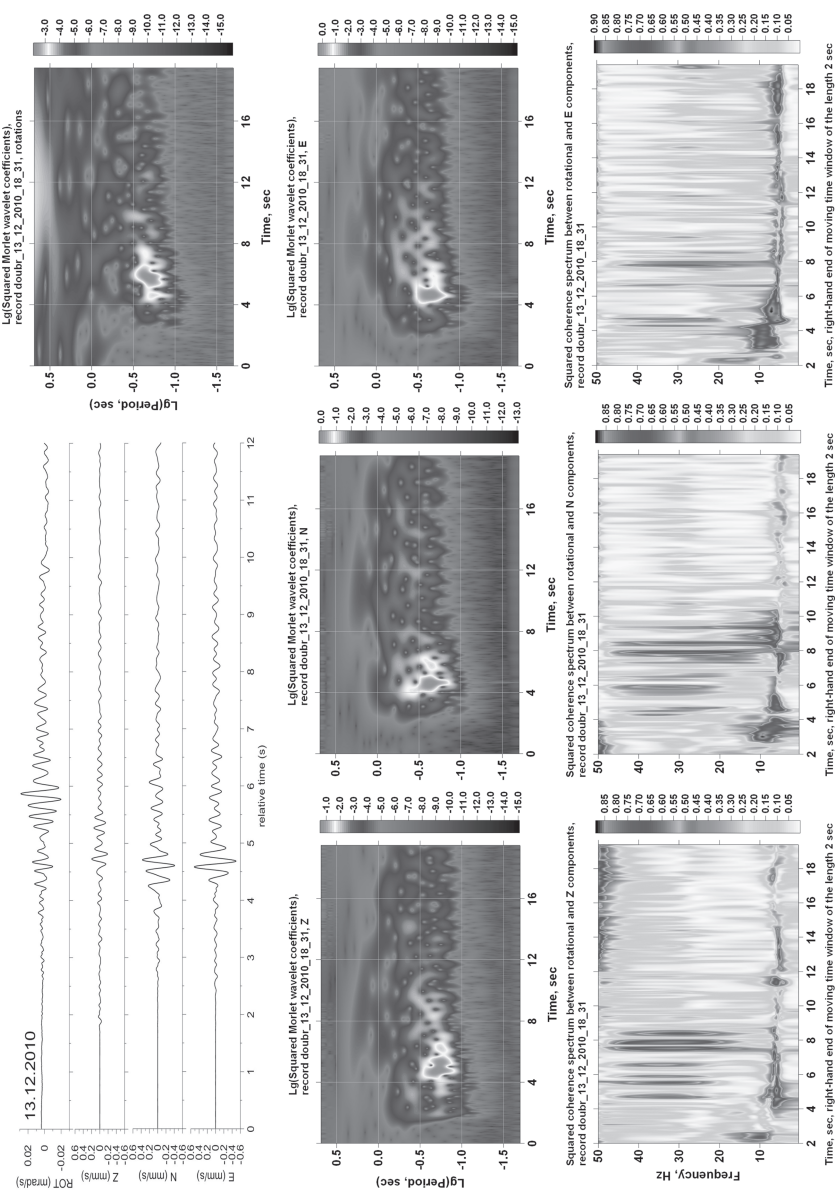

Fig. 6 Example of elaboration of "13/12" seismic event from Karviná region (for details see text and comments to Fig. 4)

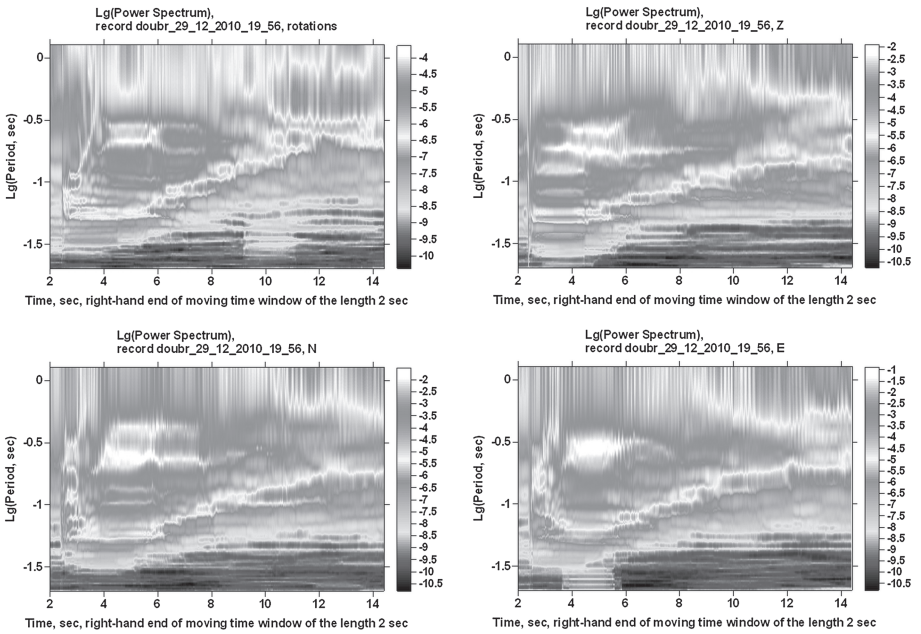

Fig. 7 Estimates of power spectra of seismic records presented at Fig. 4 within moving time window of the length 2 s

during whole elaborated time starting from rh-time 8 s, especially for "Rot, Z" and "Rot, E" components.

For estimating time-frequency spectral structure of the records we have used continuous wavelet Morlet transform. Other possibility is using estimating power spectra in short moving time window. Let us compare these two approaches for the case presented at the Fig. 4. The next Fig. 7 presents diagrams of evolution of power spectra estimates within short moving time window of the length 2 s. It could be noticed that Morlet wavelet diagrams allow more thin resolution of time structure whereas spectral estimates provide more thin frequency resolution what is quite natural.

6 Conclusion

This paper presents first results of numerical study of attributes of measured translational and rotational components of mining induced seismic events in Karviná region, Czech Republic. Squared Morlet wavelet coefficients and squared coherence spectrum between rotational and translational components were calculated for three translational components of ground vibration velocity and one rotational component of ground vibration velocity around the vertical axis.

Presented results document existence of synchronization effects between rotational and translational components for all three elaborated events with epicentral distances up to 10 km. This result documents that frequency range and prevailing frequencies of recorded wave patterns of translational and rotational components are similar. Results document that the synchronization effect is not same for all phases of seismic event. Event with epicentral distance 3 km shows coherences in P-wave phase. Two other events with epicentral distances 5

and 9 km show coherences in S-wave phase. This difference may be caused by for example focus mechanism (combination of shear and volumetric components). For presented seismic events, maximum coherences are documented in frequency range 5–20 Hz, i.e. in the prevailing frequency range of wave pattern and frequency range of used seismometers. The most significant coherence is possible to define for "Rot, E" components for all elaborated events.

Acknowledgments This research was performed with the long-term conceptual development support of research organisations RVO: 68145535 and within the frame of cooperation between Russian and Czech researchers—bilateral agreement (joint theme "Investigation of microseismic field in Ostrava-Karviná region and other areas").

References

Båth M (1979) Introduction to seismology. Birkhauser Verlag, Basel

Častová N, Kaláb Z (1997) Use of wavelet transform for processing of mining induced seismic events. In: Strakoš V, Kebo V, Farana R, Smutný L (eds) Mine planning and equipment selection 1997. Proceedings of the sixth international symposium MPES, Ostrava, A.A.Balkema/Rotterdam/Brookfield, pp 285–291

Chui CK (1992) An introduction to wavelets. Academic Press, San Diego

Daubechies I (1992) Ten lectures on wavelets. No. 61 in CBMS-NSF series in applied mathematics, SIAM, Philadelphia

Hradil P, Kaláb Z, Knejzlík J, Kořínek R, Salajka V, Kanický V (2009) Response of a panel building to mining induced seismicity in Karvina area (Czech Republic). Acta Montan Slovaca 14(2):143–151

Kaláb Z, Knejzlík J (2011) Evaluation of seismic effect generated by mining induced seismic events in Stonava area. In: Idziak AF, Dubiel R (eds) Geophysics in mining and environmental protection. Geoplanet: earth and planetary sciences, vol 2. Springer, Berlin, pp 1–10. doi:10.1007/978-3-642-19097-1_1

Kaláb Z, Knejzlík J (2012) Examples of rotational component records of mining induced seismic events from Karviná region. Acta Geodyn Geomater 9 2(166):173–178

Kaláb Z, Lednická M (2012) Foundation conditions of buildings in undermined areas: example of evaluation. Acta Geophys 60(2):399–409. doi:10.2478/s11600-011-0071-8

Kaláb Z, Knejzlík J, Lednická M (2013) Application of newly developed rotational sensor for monitoring of mining induced seismic events in the Karvina region. Acta Geodyn Geomater 10 2(170):197–205

Kaláb Z, Lednická M, Lyubushin AA (2011) Processing of mining induced seismic events by spectra analyzer software. Górnictwo i geologia Kwartalnik 6(1):75–83

Knejzlík J, Kaláb Z (2002) Seismic recording apparatus PCM3-EPC. Publ Inst Geophys Pol Acad Sci M–24(340):187–194

Knejzlík J, Kaláb Z, Rambouský Z (2012) Adaptation of the S-5-S pendulum seismometer for measurement of rotational ground motion. J Seismol 16(4):649–656. doi:10.1007/s10950-012-9279-6

Lednická M (2006) Historical buildings in the Ostrava and Karviná region and their seismic loads. Publ Inst Geophys Pol Acad Sci M–29(195):147–160

Lyubushin AA (1998) Analysis of canonical coherences in the problems of geophysical monitoring. Izv Phys Solid Earth 34:52–58

Lyubushin AA, Kaláb Z, Častová N (2004a) Application of wavelet analysis to the automatic classification of three-component seismic records. Izv Phys Solid Earth 40(7):587–593

Lyubushin AA, Pisarenko VF, Bolgov MV, Rodkin MV, Rukavishnikova TA (2004b) Synchronous variations in the Caspian Sea level from coastal observations in 1977–1991. Atmos Ocean Phys 40(6):737–746

Lyubushin AA, van Gelder PHAJM, Bolgov MV (2004) Spectral analysis of Caspian level variations. In: Proceedings of OMAE 2004: 23rd international conference offshore mechanics and arctic engineering, 20–25 June 2004, Vancouver

Lyubushin AA, Sobolev GA (2006) Multifractal measures of synchronization of microseismic oscillations in a minute range of periods. Izv Phys Solid Earth 42(9):734–744. doi:10.1134/S1069351306090035

Lyubushin AA (2008) Microseismic noise in the low frequency range (periods of 1–300 min): properties and possible prognostic features. Izv Phys Solid Earth 44(4):275–290. doi:10.1134/S1069351308040022

Lyubushin AA (2009) Synchronization trends and rhythms of multifractal parameters of the field of low-frequency microseisms. Izv Phys Solid Earth 45(5):381–394. doi:10.1134/S1069351309050024

Lyubushin AA (2010) Multifractal parameters of low-frequency microseisms. In: de Rubeis V et al. (eds) Synchronization and triggering: from fracture to earthquake processes, GeoPlanet: Earth and Planetary Sciences 1, Springer, Berlin, Chapter 15, pp 253–272. doi:10.1007/978-3-642-12300-9_15

Lyubushin AA, Klyashtorin LB (2012) Short term global *dT* prediction using (60–70)-years periodicity. Energy Environ 23(1):75–85

Lyubushin AA (2014) Analysis of coherence in global seismic noise for 1997–2012. Izv Phys Solid Earth 50(3):325–333. doi:10.1134/S1069351314030069

Mallat S (1998) A wavelet tour of signal processing. Academic Press, San Diego

Marple SL Jr (1987) Digital spectral analysis with applications. Prentice-Hall Inc, Englewood Cliffs

Martinec P et al (2006) Termination of underground coal mining and its impact on the environment. Anagram, Ostrava

Teisseyre R, Takeo M, Majewski E (eds) (2006) Earthquake source asymmetry, structural media, and rotation effects. Springer, Berlin